The Role of the NOD1/Rip2 Signaling Pathway in Myocardial Remodeling in Spontaneously Hypertensive Rats

Authors' Contribution:
Study Design A
Data Collection B
Statistical Analysis C
Data Interpretation D
Manuscript Preparation E
Literature Search F
Funds Collection G

ABCEF 1 **Feng-Yi Liu***
ABCDEF 1,2 **Bing-Qian Fang**
BDF 3 **Ling-Min Sun**
BCF 3 **Xiu-Zhen Zhang**
ABCDF 1 **Jin-Li Liu**
BCDF 4 **Yun Yang**
BCDF 4 **Wen-Hua Zhang**
BCDF 3 **Xiu-Li Wang**
ABCDEFG 1 **Yan-Chun Ding**

1 Department of Cardiology V, The Second Affiliated Hospital of Dalian Medical University, Dalian, Liaoning, P.R. China
2 Department of Internal Medicine, Shaoxing Central Hospital, Shaoxing, Zhejiang, P.R. China
3 College of Basic Medical Sciences, Dalian Medical University, Dalian, Liaoning, P.R. China
4 Department of Ultrasound, The Second Affiliated Hospital of Dalian Medical University, Dalian, Liaoning, P.R. China

Corresponding Author:
Source of support:

* Feng-Yi Liu and Bing-Qian Fang contributed equally
Yan-Chun Ding, e-mail: yanchunding@aliyun.com
This work was supported by Liaoning Provincial Natural Science Foundation Project (Project No.: 2014023015)

Background: Chronic hypertension changes the function and structure of the heart and blood vessels. This study aimed to explore the role of the NOD1/Rip2 (nucleotide-binding oligomerization domain 1/receptor-interacting protein 2) signaling pathway in myocardial remodeling in spontaneously hypertensive rats (SHRs).

Material/Methods: Blood pressure was measured using a tail cuff. The cardiac structure was observed using echocardiography. Slices of the myocardium were stained with hematoxylin and eosin. The expression of NOD1 and Rip2 was detected using real-time polymerase chain reaction, western blot, and immunohistochemistry. The content and distribution of collagen in the myocardium were observed using Van Gieson staining. Enzyme-linked immunosorbent assay was used to detect the interleukin-1 (IL-1) concentrations. SHRs were treated with the NOD1 agonist iE-DAP and NOD1 inhibitor ML130.

Results: The NOD1 agonist increased blood pressure in SHRs, and the NOD1 inhibitor decreased blood pressure; the interventricular septum thickness (IVST) and left ventricular posterior wall thickness (LVPWT) of the agonist-treated group were thicker than those of the control group, and the antagonist exerted the opposite effects. The levels of the NOD1 and Rip2 mRNAs and proteins, serum IL-1 concentration, and myocardial collagen volume fraction (CVF%) increased in SHRs in the NOD1 agonist group, but the levels of NOD1 and Rip2, serum IL-1 concentration, and myocardial collagen volume fraction (CVF%) decreased in SHRs in the NOD1 inhibitor group.

Conclusions: NOD1/Rip2 expression increased during the progression of myocardial remodeling in SHRs. The NOD1 agonist increased NOD1 expression and promoted myocardial remodeling, while the NOD1 antagonist reduced NOD1/Rip2 expression and protected against myocardial remodeling.

MeSH Keywords: Hypertension • Inflammation • Nod1 Signaling Adaptor Protein • Ventricular Remodeling

Full-text PDF: https://www.medscimonit.com/abstract/index/idArt/924748

📄 4508   ▦ 1   📊 10   📖 50

Background

Hypertension is a cardiovascular syndrome. Left ventricular hypertrophy and vascular remodeling are 2 types of damage in target organs in individuals with hypertension, which is closely related to the occurrence of arrhythmia, sudden death, heart failure, and other complications in patients with hypertension. Approximately one-third of hypertensive patients exhibit left ventricular remodeling [1]. The most commonly used drugs for improving myocardial remodeling are β-blockers, renin-angiotensin system inhibitors, and aldosterone receptor antagonists. Many studies have confirmed that some new therapies improve myocardial remodeling, including the angiotensin II receptor blocker losartan, mineralocorticoid receptor blocker spironolactone, 3-hydroxy-3-methyglutaryl-coenzyme A reductase inhibitors simvastatin and atorvastatin, and N-acetylcysteine [2]. Also, many researchers have introduced 3-dimensional graphene foams which provide a new research direction for myocardial cell regeneration [3]. According to a meta-analysis, antihypertensive therapy prevents cardiovascular disease and death [4]. Thus, the pathogenesis of hypertension has become the key research area investigated by many scholars.

The innate immune system, as the first line of the body's defenses, plays an important role in the pathogenesis of many inflammatory diseases [5]. Many studies have also confirmed that the innate immune response is related to some cardiovascular diseases [6]. The innate immune system detects various pathogen-associated molecular patterns (PAMP) through pattern recognition receptors (PRRs) [7]. The nucleotide-binding oligomerization domain (NOD)-like receptor (NLR) family is one type of innate immune receptor, and some receptors are involved in a series of reactions after myocardial injury [8–10].

The NOD receptor plays an important role in regulating the inflammatory response of the body and participates in the occurrence and development of many chronic inflammatory diseases, including atherosclerosis [11]. NOD1 is expressed in the heart [12,13], and NOD1 expression is upregulated in both human and mouse heart failure models, while cardiac function and cardiac remodeling are improved in mice lacking the NOD1 gene [10], indicating that NOD1 is involved in the process of myocardial remodeling. NOD1 oligomerization induced by binding to peptidoglycan fragments leads to the recruitment and activation of receptor-interacting protein 2 (Rip2) [14], and activation of NOD1/Rip2 signaling further activates nuclear factor-κB and promotes the production of inflammatory factors [15–18].

However, the roles of NOD1 in the pathogenesis of hypertension and myocardial remodeling induced by hypertension are unclear. In this study, we observed the expression of genes and proteins associated with the NOD1/Rip2 signaling pathway during myocardial remodeling in spontaneously hypertensive rats (SHRs), and then explored the role of the NOD1/Rip2 signaling pathway in SHR myocardial remodeling, with the aim of identifying new targets for the prevention and control of hypertension-induced target organ damage.

Material and Methods

Animals and reagents

This study analyzed 5 healthy male Wistar-Kyoto (WKY) rats each at 8, 12, and 16 weeks of age, 5 SHRs each at 12 and 16 weeks of age, and 20 SHRs at 8 weeks of age. The animals were purchased from Beijing Weitong Lihua Animal Technology Co., Ltd. (License: SCXK(jing)2012-0001), and housed in the specific pathogen free (SPF) barrier system at the Animal Research Institute of Genetic Engineering for Major Diseases of Dalian Medical University (License: SYXK(liao)2013-0006). All procedures using animals conformed to the National Regulations on the Administration of Laboratory Animals. At the end of the experiment, the rats were euthanized with excess chloral hydrate until respiration and heartbeats were not observed.

Rabbit NOD1 and Rip2 polyclonal antibodies were purchased from Santa Cruz. The β-actin monoclonal antibody was purchased from the ProteinTech Group. The HRP-conjugated goat anti-rabbit IgG secondary antibody was purchased from Beijing Boos. The NOD1 receptor agonist iE-DAP was purchased from InvivoGen, and the NOD1 inhibitor ML130 (ab142177) was purchased from Abcam. The Van Gieson (VG) trichrome staining solution was obtained from Solarbio. The Immunohistochemical staining kit SP-9000 and iE-DAP were purchased from Beijing Zhongzhuang Jinqiao. The interleukin-1 (IL-1) ELISA kit was purchased from Shanghai Longton ELISA Reagent Company.

Experimental group

The experiment was divided into 2 parts. The first part was designed to detect the changes in the expression of the NOD1 and Rip2 mRNAs and proteins in SHR and Wistar-Kyoto (WKY) rats at different ages. In the second part, 8-week-old male SHRs were randomly divided into 4 groups: the SHR-H group that was administered the NOD1 receptor-specific agonist iE-DAP (350 μg/100 g), the SHR-I group that was administered the NOD1 receptor-specific inhibitor ML-130 (100 μg/100 g), the SHR-NS group that was administered an equal amount of normal saline, and the SHR-C group of SHRs at the same age as the control group. The experiment was performed after adaptive feeding at the SPF center for 1 week. Agonists and inhibitors were injected intraperitoneally every other day for 7 total injections. After 1 week of feeding, tissues and blood samples were collected separately.

Blood pressure measurement method

We used a caudal cuff method to measure blood pressure in awake rats using an automatic noninvasive blood pressure measurement system for rats (Chengdu Taimeng). The rats were fixed in the cage with their abdominal wall facing downward. The temperature in the experiment box was maintained at a constant value of 32°C, and the experimental room was kept quiet at all times. The rat tail passed through the pulse blocker to block the rat caudal artery. After the sensor was correctly fixed to the occluder, BP-300A software was initiated and the blood pressure was measured after the stable pulse waveform appeared in the monitoring software. The systolic blood pressure (SBP) and diastolic blood pressure (DBP) were calculated through computerized curve fitting. Each rat was tested 5 times, and the average values were recorded.

Echocardiographic analysis

Rats were fixed on the plank in the supine position under 10% chloral hydrate (300 mg/kg, intraperitoneal injection) anesthesia, and then the chest hair was shaved. After the rats were inclined to the left at 30°, we placed the Siemens ACUSON Sequoia 512 ultrasonic diagnostic probe with frequency of 5–10 MHZ on the left side of the sternum. The probe was located at an angle of 10° to 30° to the central line of the sternum to display the long axis section of the sternum, and then rotated 90° clockwise to show the short axis section of the left ventricle. The acoustic beam was placed perpendicular to the left ventricular cavity to ensure that the cutting plane of the left ventricular cavity was as circular as possible. M-mode echocardiograms were obtained from the M sampling line perpendicular to septum and posterior wall of left ventricle at the papillary muscle level. M-type curves were guided and measured by capturing 2-dimensional images. According to the method recommended by the American College of Echocardiography (ASE), the average value of 3 cardiac cycles was recorded for images from each rat. The echocardiographic measures were the left ventricular end diastolic diameter (LVDd), left ventricular end systolic diameter (LVDs), interventricular septum thickness (IVST), and left ventricular posterior wall thickness (LVPWT). The ultrasonic measurements were the LVDd, LVDs, IVST, and LVPWT. Using the Teichholtz formula, $V=7.0/(2.4+D)\times D^3$, the left ventricular end-diastolic volume (LVEDV) and end-systolic volume (LVESV) were calculated from the LVDd and LVDs, respectively. The following equations were used to calculate other parameters: stroke volume (SV)=LVEDV-LVESV, cardiac output (CO)=SV×HR, left ventricular ejection fraction (EF)=SV/LVEDV×100%, and left ventricular shortening rate (FS)=(LVDd-LVDs)/LVDd×100%. The measurement data are reported as the means±standard deviations ($\chi\pm s$).

Table 1. Rat primer sequence list.

Gene		Primer sequence
NOD1	Forward	5'-TAGCCTTCTGCAATGCTTGTTC-3'
	Reverse	5'-CCGTGAGACGGCTAAAGCAA-3'
Rip2	Forward	5'-CGTCGAAGGCGTACCATTG-3'
	Reverse	5'-GTGGGCGCTCTGAACTTTTC-3'
β-actin	Forward	5'-CCTGTGGCATCCATGAAACTAC-3'
	Reverse	5'-CCAGGGCAGTAATCTCCTTCTG-3'

H&E staining

Rats under 10% chloral hydrate (300 mg/kg, intraperitoneal injection) anesthesia did not display signs of peritonitis, pain, or discomfort. A ventral midline incision was created, and blood was collected from the abdominal aorta of each rat with a blood sampling needle. Myocardial tissue was separated quickly after blood was removed and washed with phosphate buffered saline (PBS). The apex was fixed with 10% of formalin for 24 hours, and then embedded in paraffin. Sections were cut at a thickness of 5 μm. The tissue was stained with H&E, and myocardial remodeling was observed under an inverted phase contrast microscope.

Real time polymerase chain reaction (RT-PCR)

Total RNA was extracted from the myocardial tissue using RNA extraction kit (Beijing Whole Golden Organism) and then reverse transcribed to synthesize cDNAs, which were detected using an MX-3000P fluorescence quantitative polymerase chain reaction (PCR) instrument. Rat primer sequences were synthesized by Invitrogen Company, as shown in Table 1. The reaction system was 20 μL, including 10 μL of SYBR Premix, 0.4 μL of ROX, 2 μL of cDNAs, and 5.6 μL of RNase-free water. Using β-actin as a reference, we used the comparative cycle threshold method to analyze the relative levels of the NOD1 and Rip2 mRNAs in the samples.

Western blot

Myocardial tissue samples were collected on ice to prevent protein degradation. After adding a protein lysis solution, samples were ultrasonicated and centrifuged. The supernatant was collected and the total protein content was determined. The protein concentration was calculated from the absorbance value of the sample to be measured after generating a protein standard curve. After electrophoresis, transferring proteins to the membrane, incubation with the primary antibody, washing, incubation with the secondary antibody, and exposure, we used the ImageJ gray scale analysis software to analyze the exposed films. The ratio of the gray value of the final target protein to β-actin was calculated as an index of its expression level.
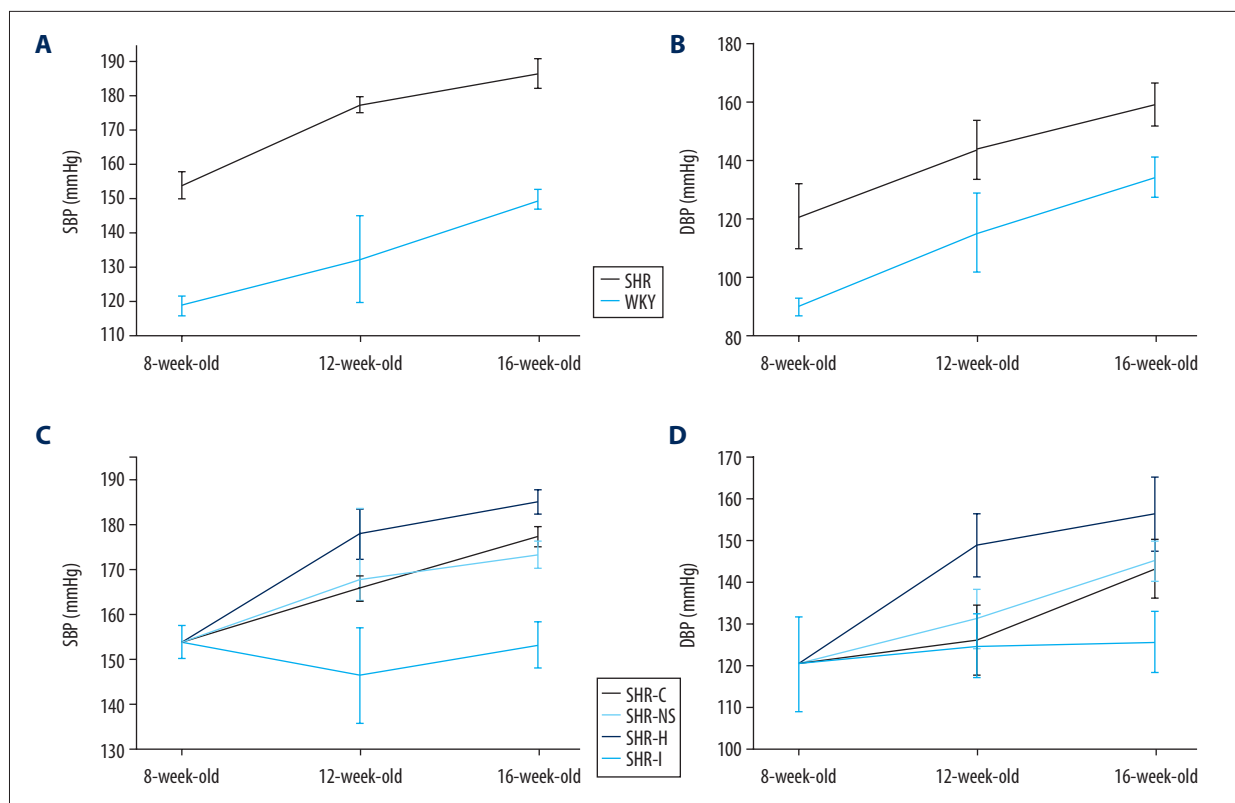
Figure 1. (**A, B**) Comparison of blood pressure between SHR and WKY rats of the same ages. (**C, D**) The effects of NOD1 agonists and inhibitors on blood pressure in SHRs. SHRs – spontaneously hypertensive rats; WKY – Wistar-Kyoto; NOD1 – nucleotide-binding oligomerization domain 1.

Immunohistochemical staining

Myocardial tissue was treated as described and cut uniformly after being embedded in paraffin. Sections were subjected to conventional dewaxing, rehydration, high pressure repair, sealing, incubations with the primary and secondary antibodies, and stained with DAB. Then, immunohistochemical staining for NOD1 and Rip2 in the myocardium was observed under an inverted phase contrast microscope. NOD1- and Rip2-positive signals were brown and located in the cytoplasm of cells. We performed a semiquantitative analysis to evaluate the expression of NOD1 and Rip2. The grayscale value of immunohistochemical staining in myocardial slices from each group was measured using the image signal acquisition and analysis software ipp6.0, and visual fields of each sample were imaged at a 40× magnification. Three visual fields were randomly selected. The gray value indicated the expression of the corresponding protein, and the average value was recorded.

Enzyme-linked immunosorbent assay (ELISA)

We collected 5 mL of blood from the abdominal aorta. The concentrations of inflammatory factors in the samples were determined using enzyme-linked immunosorbent assay (ELISA).

The concentration of the inflammatory factor IL-1 was calculated after creating a standard curve.

Van Gieson (VG) staining

The content and distribution of collagen in the myocardium were observed using Van Gieson (VG) staining. The collagen fibers were bright red, muscle fibers, glial cells and erythrocytes were yellow, and the nuclei were blue. Using the Brilla method, we measured the myocardial collagen volume fraction (CVF%)=left ventricular collagen area/visual field area ×100% from 5 randomly selected visual fields, and the mean value was obtained.

Statistical analysis

The data were statistically analyzed using SPSS18.0 software. The measurement data are presented as the means±standard deviations (χ±s). One-way analysis of variance was used to compare the data within groups, and t-test was used to compare the data between the 2 groups. Dunnett's T3 test was used for post hoc subgroup analyses. The difference was considered statistically significant when $P<0.05$.
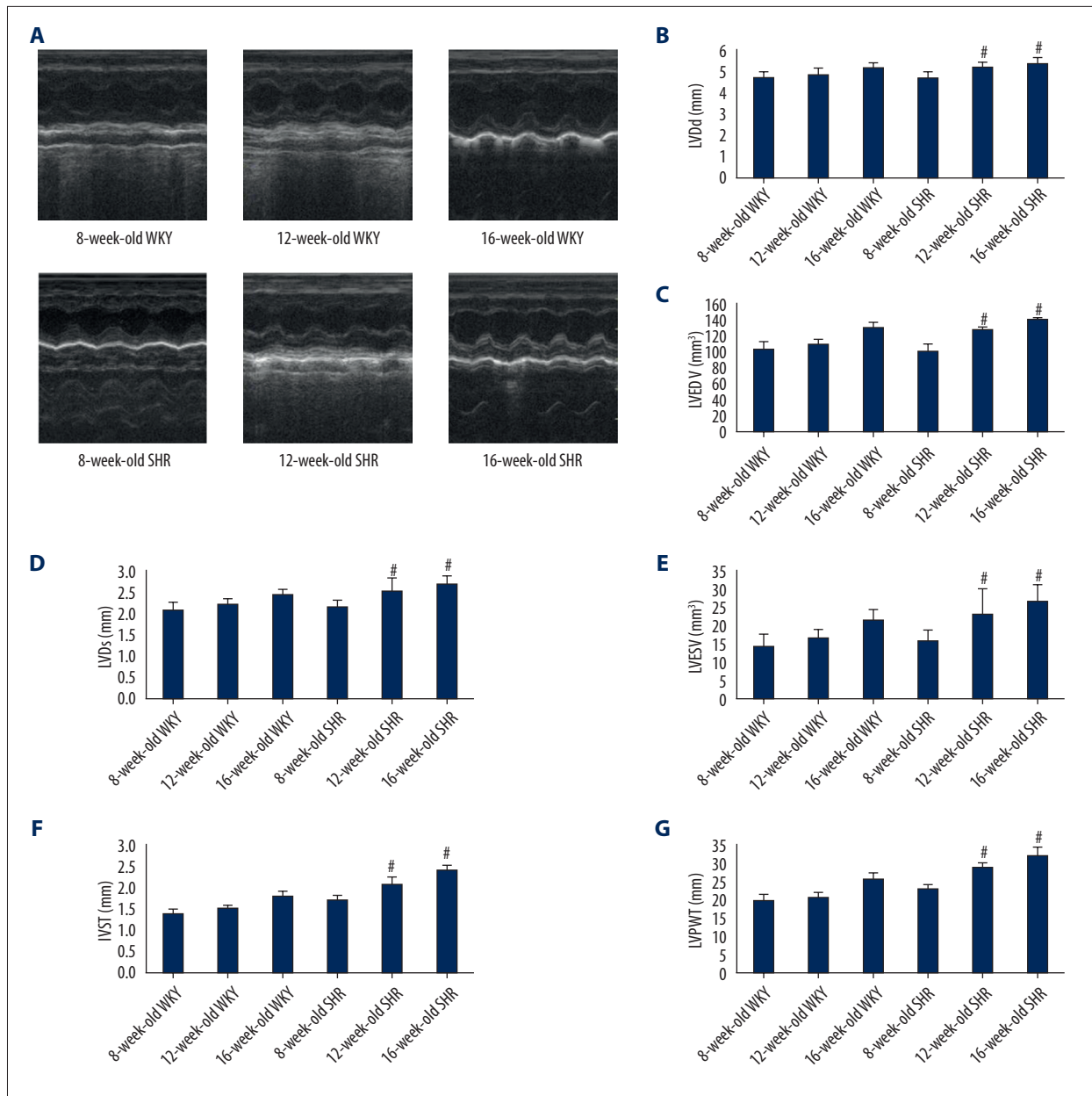
e924748-4

Indexed in: [Current Contents/Clinical Medicine]   [SCI Expanded]   [ISI Alerting System]
[ISI Journals Master List]   [Index Medicus/MEDLINE]   [EMBASE/Excerpta Medica]
[Chemical Abstracts/CAS]

Figure 2. (**A**) Cardiac echocardiographic cycle in rats of different ages. (**B–G**) LVDd, LVEDV, LVDs, LVESV, IVST, and LVPWT in WKY rats and SHRs. * *P*<0.05 compared with 16-week-old WKY rats, and # *P*<0.05 compared with 8-week-old SHRs. SHRs – spontaneously hypertensive rats; WKY – Wistar-Kyoto; LVDd – left ventricular end diastolic diameter; LVEDV – left ventricular end-diastolic volume; LVDs – left ventricular end systolic diameter; LVESV – left ventricular end-systolic volume; IVST – interventricular septum thickness; LVPWT – left ventricular posterior wall thickness.

Results

Effects of NOD1 agonists and inhibitors on the blood pressure of SHRs

The blood pressure of SHRs and WKY rats increased with aging, but the blood pressure of SHRs was significantly higher than the WKY rats of the same age (*P*<0.05, Figure 1A, 1B).

Rats were divided into 4 groups to observe the effects of NOD1 agonists and inhibitors on the blood pressure of SHRs: a control group (SHR-C group), saline injection group (SHR-NS group), NOD1 agonist group (SHR-H group), and NOD1 inhibitor group (SHR-I group). The blood pressure increased significantly in the SHR-H, SHR-NS, and SHR-C groups with aging, but not in the SHR-I group. At 12 weeks, significantly higher SBP and DBP were observed in the SHR-H group than in the
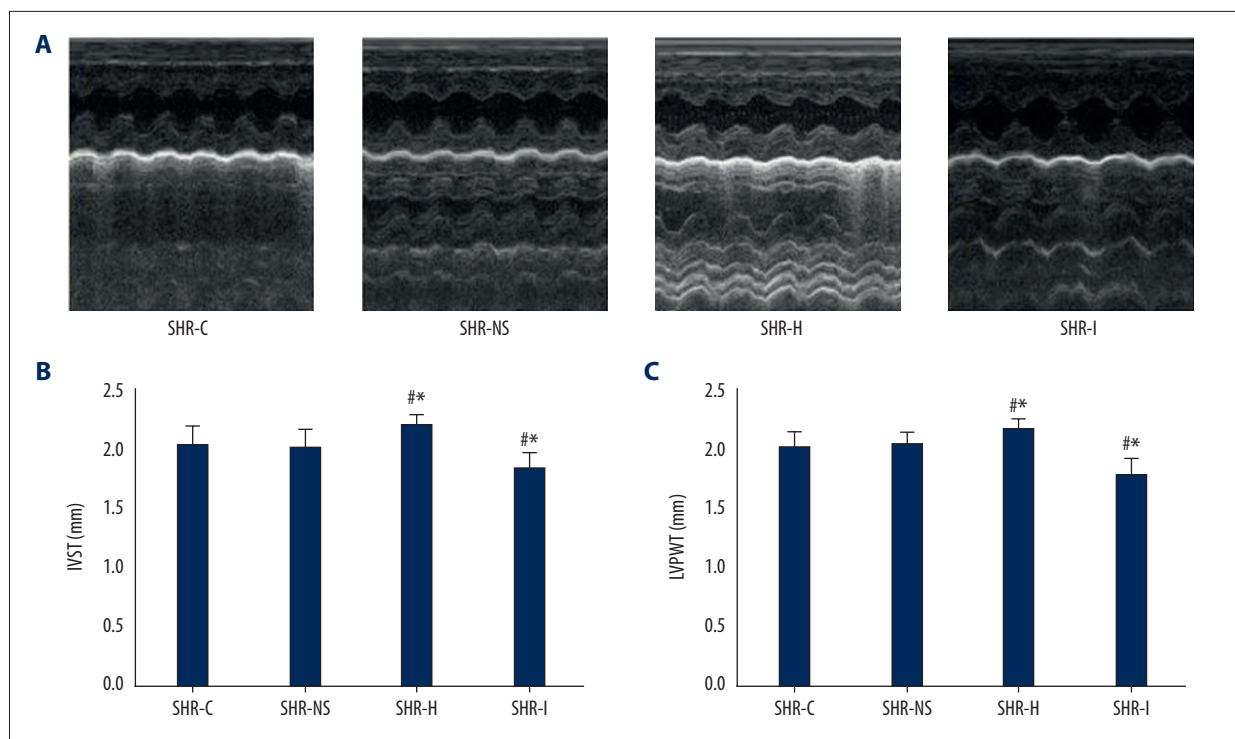
Figure 3. (**A**) Cardiac echocardiography cycle in each experimental group. (**B, C**) IVST and LVPWT in each experimental group. * $P<0.05$ compared with the SHR-C group, and # $P<0.05$ compared with the SHR-NS group. IVST – interventricular septum thickness; LVPWT – left ventricular posterior wall thickness; SHRs – spontaneously hypertensive rats; SHR-C group – control group; SHR-NS group – saline injection group.

SHR-NS and SHR-C groups ($P<0.05$, Figure 1C, 1D), but significantly lower SBP and DBP were observed in the SHR-I group than in the SHR-NS and SHR-C groups ($P<0.05$, Figure 1C, 1D). Thus, NOD1 agonists significantly increased the blood pressure of SHRs, while NOD1 inhibitors inhibited the elevation in the blood pressure of SHRs. NOD1 may be involved in the process of increased blood pressure in SHRs.

The echocardiographic analysis of myocardial remodeling in rats

Using the ASE method, the mean values of 3 cardiac cycles in rats were recorded using echocardiography in rats of different ages (Figure 2A). As shown in Figure 2F, 2G, the IVST and LVPWT of SHRs and WKY rats increased with aging. Compared with 16-week-old WKY rats and 8-week-old SHRs, IVST and LVPWT were significantly thicker and myocardial remodeling was more obvious in 16-week-old SHRs. The differences in LVDd, LVEDV, LVDs, and LVESV in SHRs at different ages were statistically significant ($P<0.05$, Figure 2B–2E). No significant differences in SV, CO, FS, and EF were observed ($P>0.05$).

SHRs were randomly divided into 4 groups: the SHR-H group, SHR-I group, SHR-NS group, and SHR-C group. Cardiac echocardiography cycles were measured in each experimental

group (Figure 3A). The results of echocardiography in each group did not reveal significant differences in LVDd, LVEDV, LVDs, LVESV, SV, FS%, and EF% between the 4 groups. As shown in Figure 3B , 3C, the IVST and LVPWT of SHR-H group were thicker than the SHR-C group and SHR-NS group, but the IVST and LVPWT of the SHR-I group were not thicker than the SHR-C group and SHR-NS group. Based on these results, NOD1 agonists promoted myocardial remodeling in SHRs, while NOD1 inhibitors blocked this process.

Observation of H&E staining in the isolated rat myocardium

We observed the condition of the rat myocardium by performing H&E staining. Compared with 16-week-old WKY rats, 8-week-old SHRs and 12-week-old SHRs, the myocardial cells of 16-week-old SHRs were significantly larger, some of the fibers were broken, the cytoplasm was dissolved and necrotic, and the boundary was blurred (Figure 4A). As shown in Figure 4B, compared with the SHR-C group, the structure of the myocardial tissue in the SHR-I group was significantly improved, while cardiomyocytes were significantly enlarged and the structure was disrupted in the SHR-H group.
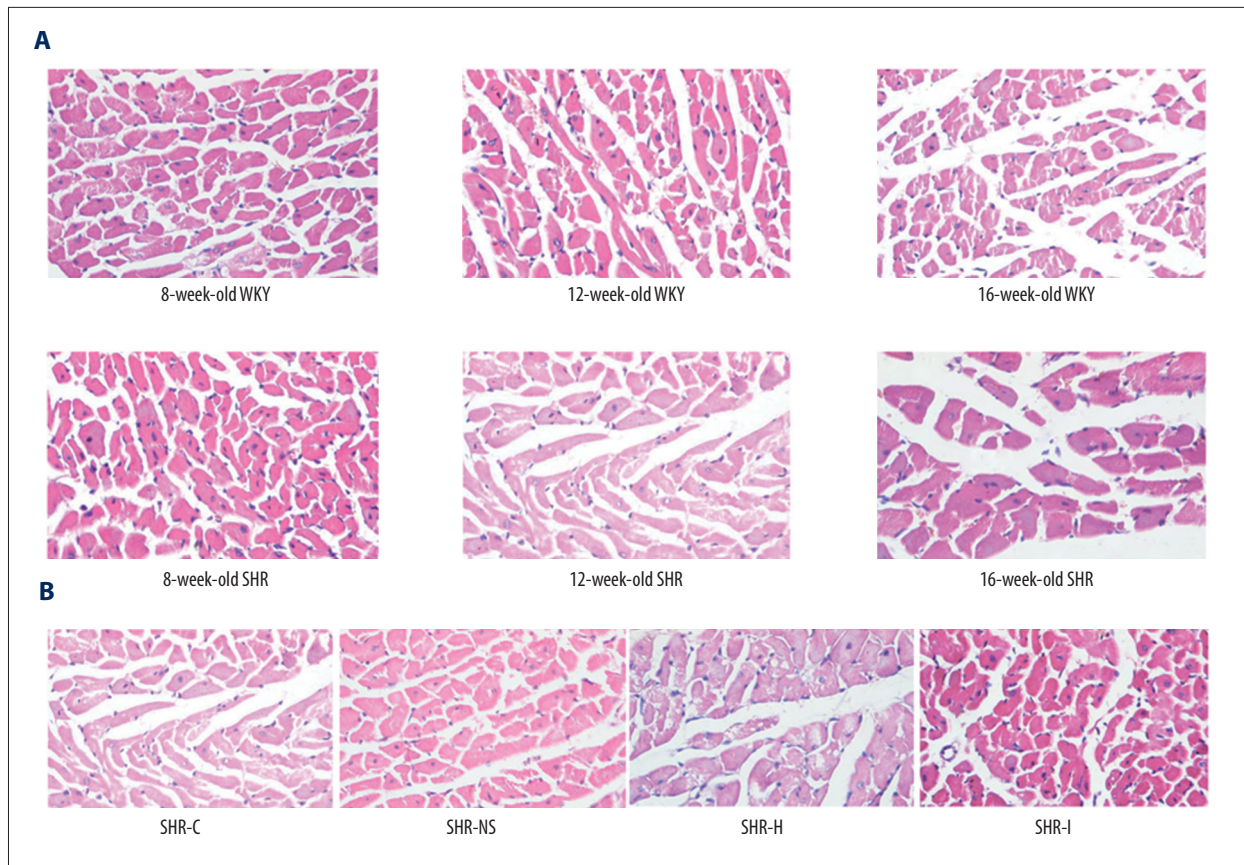
Figure 4. (**A**) Images of hematoxylin and eosin (H&E) staining of the myocardial tissue from rats of different ages. (**B**) Images of H&E staining of the myocardial tissue from rats in each experimental group.

Determination of the expression of the NOD1 and Rip2 mRNAs in the rat myocardium using RT-PCR

The RT-PCR analysis revealed increased expression of the NOD1 and Rip2 mRNAs in myocardial tissue of SHRs with aging. The relative expression of NOD1 in 16-week-old SHRs was 3.15 times greater than in 8-week-old SHRs, and the relative expression of NOD1 in 12-week-old SHRs was 2.06 times greater than 8-week-old SHRs; the differences were significant ($P<0.05$, Figure 5A). The relative expression of Rip2 in 16-week-old SHRs was 1.96 times greater than in 8-week-old SHRs, and the relative expression of Rip2 in 12-week-old SHRs was 1.42 times greater than in 8-week-old SHRs ($P<0.05$, Figure 5B). The expression of the NOD1 and Rip2 mRNAs in the myocardial tissue of WKY rats did not increase with aging, and no significant differences in the expression of these mRNAs were observed in WKY rats of different ages ($P>0.05$, Figure 5A, 5B). The relative expression of the NOD1 and Rip2 mRNAs in the myocardial tissue of 16-week-old SHRs was significantly higher than in 16-week-old WKY rats ($P<0.05$, Figure 5A, 5B). Thus, the expression of the NOD1 and Rip2 mRNAs increased during myocardial remodeling in SHRs.

When agonists and inhibitors were administered to each experimental group, the relative expression of the NOD1 and Rip2 mRNAs in the SHR-H group was significantly higher than in the SHR-C and SHR-NS groups ($P<0.05$, Figure 5C, 5D). The NOD1 and Rip2 mRNAs were expressed at significantly lower levels in the SHR-I group than in the SHR-C and SHR-NS groups ($P<0.05$, Figure 5C, 5D). Based on these findings, the NOD1 agonist upregulated the expression of the NOD1 and Rip2 mRNAs in the myocardium of SHRs, while the NOD1 inhibitor decreased the expression of the NOD1 and Rip2 mRNAs.

Determination of NOD1 and Rip2 protein in rat myocardium by western blot

As shown in Figure 6A–6C, the western blot analysis showed increased levels of the NOD1 and Rip2 proteins in the myocardial tissue of SHRs with aging, and higher relative levels of NOD1 and Rip2 were observed in 16-week-old SHRs than in 8-week-old SHRs. The difference was statistically significant ($P<0.05$). The levels of the NOD1 and Rip2 proteins in the myocardial tissue of WKY rats did not increase with aging, and significant differences were not observed between 8-, 12- and 16-week-old WKY rats ($P>0.05$). The NOD1 and Rip2 proteins
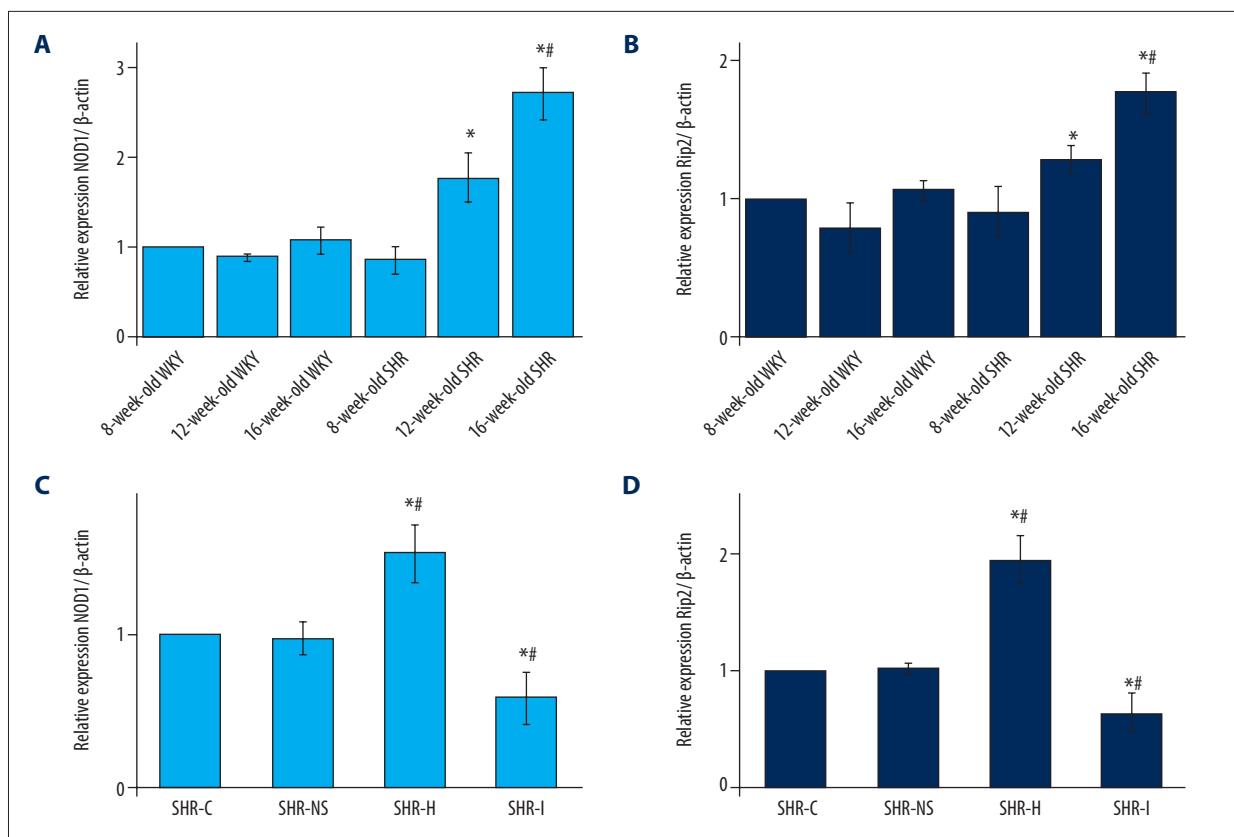
Figure 5. (**A, B**) Expression of the NOD1 and Rip2 mRNAs in the myocardium of SHRs rats and WKY rats of different ages. * *P*<0.05 compared with the 8-week-old SHRs, and # *P*<0.05 compared with the 8-week-old WKY rats. (**C, D**) Expression of the NOD1 and Rip2 mRNAs in the rat myocardium. * *P*<0.05 compared with the SHR-C group, and # *P*<0.05 compared with the SHR-NS group. NOD1 – nucleotide-binding oligomerization domain 1; Rip2 – receptor-interacting protein 2; mRNAs – messenger RNAs; SHRs – spontaneously hypertensive rats; WKY – Wistar-Kyoto; SHR-C group – control group; SHR-NS group – saline injection group.

were expressed at significantly higher levels in the myocardial tissue of 16-week-old SHRs than in WKY rats of the same age (*P*<0.05). Levels of the NOD1 and Rip2 proteins increased during myocardial remodeling in SHRs.

When agonists and inhibitors were administered to each experimental group, higher relative levels of the NOD1 and Rip2 proteins were observed in the SHR-H group than in the SHR-C and SHR-NS groups (*P*<0.05, Figure 6D–6F). However, significantly lower levels of the NOD1 and Rip2 proteins were detected in the SHR-I group than in the SHR-C and SHR-NS groups (*P*<0.05, Figure 6D–6F). The NOD1 agonist increased the levels of the NOD1 and Rip2 proteins in the myocardium of SHRs, while the NOD1 inhibitor decreased the levels of the NOD1 and Rip2 proteins.

Immunohistochemical staining for the NOD1 and Rip2 proteins in the rat myocardium

We observed the changes in the expression of the NOD1 and Rip2 proteins expression in the rat myocardium using immunohistochemical staining, and we performed a semiquantitative analysis of myocardial immunohistochemical staining under an inverted phase contrast microscope. Significantly higher expression of the NOD1 and Rip2 proteins was observed in the myocardium of 16-week-old SHRs than in 8-week-old SHRs (*P*<0.05). However, the expression of the NOD1 and Rip2 proteins in 16-week-old WKY rats did not significantly differ from 8-week-old and 12-week-old WKY rats (*P*>0.05, Figure 7).

After treatment with agonists and inhibitors, significantly higher expression of the NOD1 and Rip2 proteins was observed in the SHR-H group than in the SHR-C group and SHR-NS groups (*P*<0.05). The expression of the NOD1 and Rip2 proteins was significantly decreased in the in SHR-I group, and the difference was statistically significant (*P*<0.05, Figure 8).
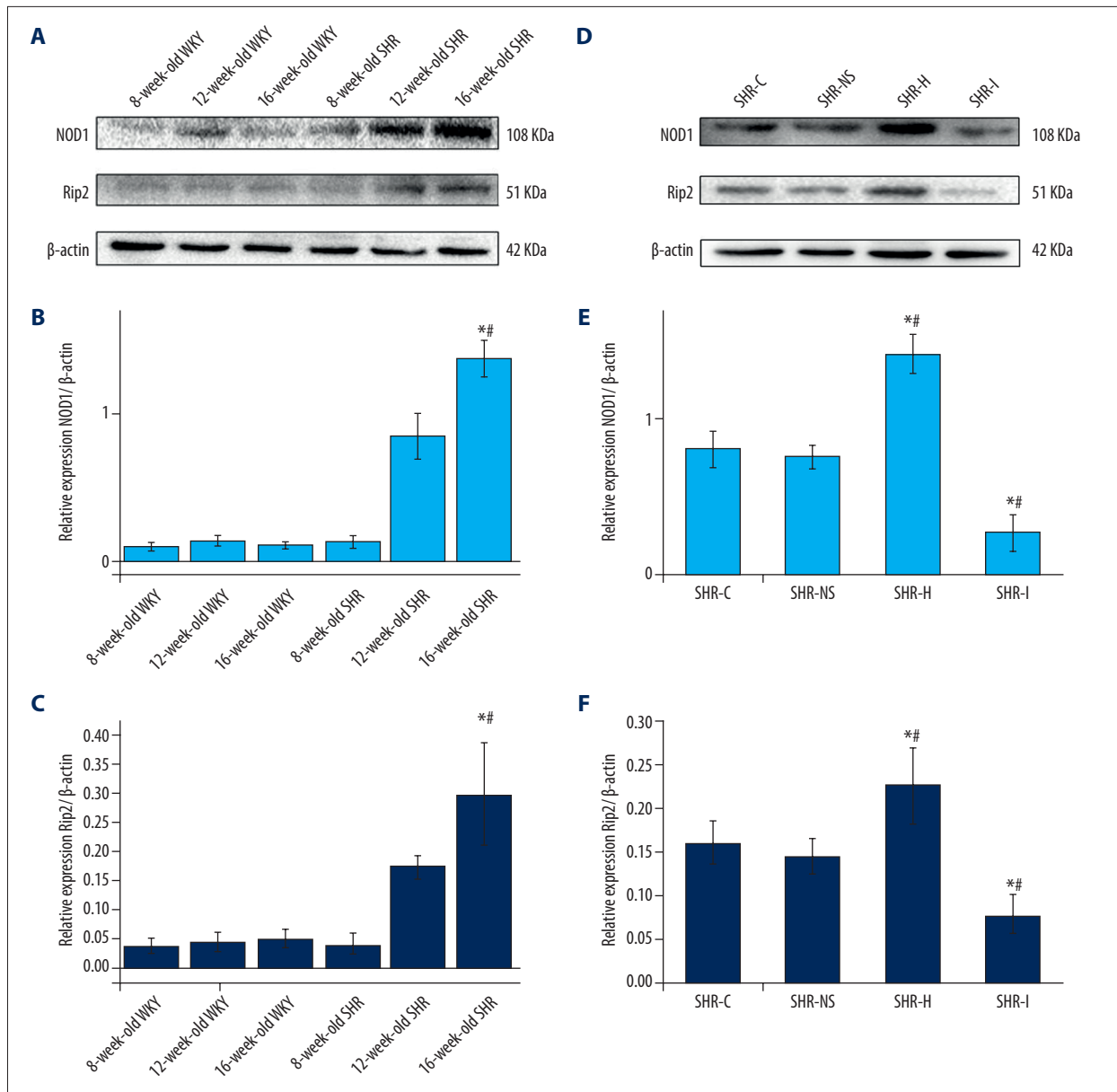
Figure 6. (**A–C**) Western blots showing the levels of the NOD1 and Rip2 proteins in the myocardium of SHRs and WKY rats. * $P < 0.05$ compared with the 8-week-old SHRs, and # $P < 0.05$ compared with the 16-week-old WKY rats. (**D–F**) Western blots showing the levels of the NOD1 and Rip2 proteins in the myocardium of SHRs in each experimental group. * $P < 0.05$ compared with the SHR-C group, and # P 0.05 compared with the SHR-NS group. NOD1 – nucleotide-binding oligomerization domain 1; Rip2 – receptor-interacting protein 2; SHRs – spontaneously hypertensive rats; WKY – Wistar-Kyoto; SHR-C group – control group; SHR-NS group – saline injection group.

Detection of the collagen content in the rat myocardium using VG staining

Collagen was distributed in the interstitial and perivascular myocardium of 16-week-old SHRs. Compared with WKY rats of the same age, the number of myocardial collagen fibers increased significantly and exhibited a disordered arrangement. The results of the semiquantitative analysis of VG staining are shown in Figure 9A and 9C. The number of myocardial collagen fibers increased significantly in 16-week-old SHRs. The CVF% was 3.65 times higher in 16-week-old SHRs than in 8-week-old SHRs, and the CVF% was 2.3 times higher in 12-week-old SHRs than in 8-week-old SHRs. The difference was statistically significant ($P < 0.05$). The results of the semiquantitative analysis of VG staining in each experimental group are shown in Figure 9B and 9D. Compared with the SHR-C group, the CVF%
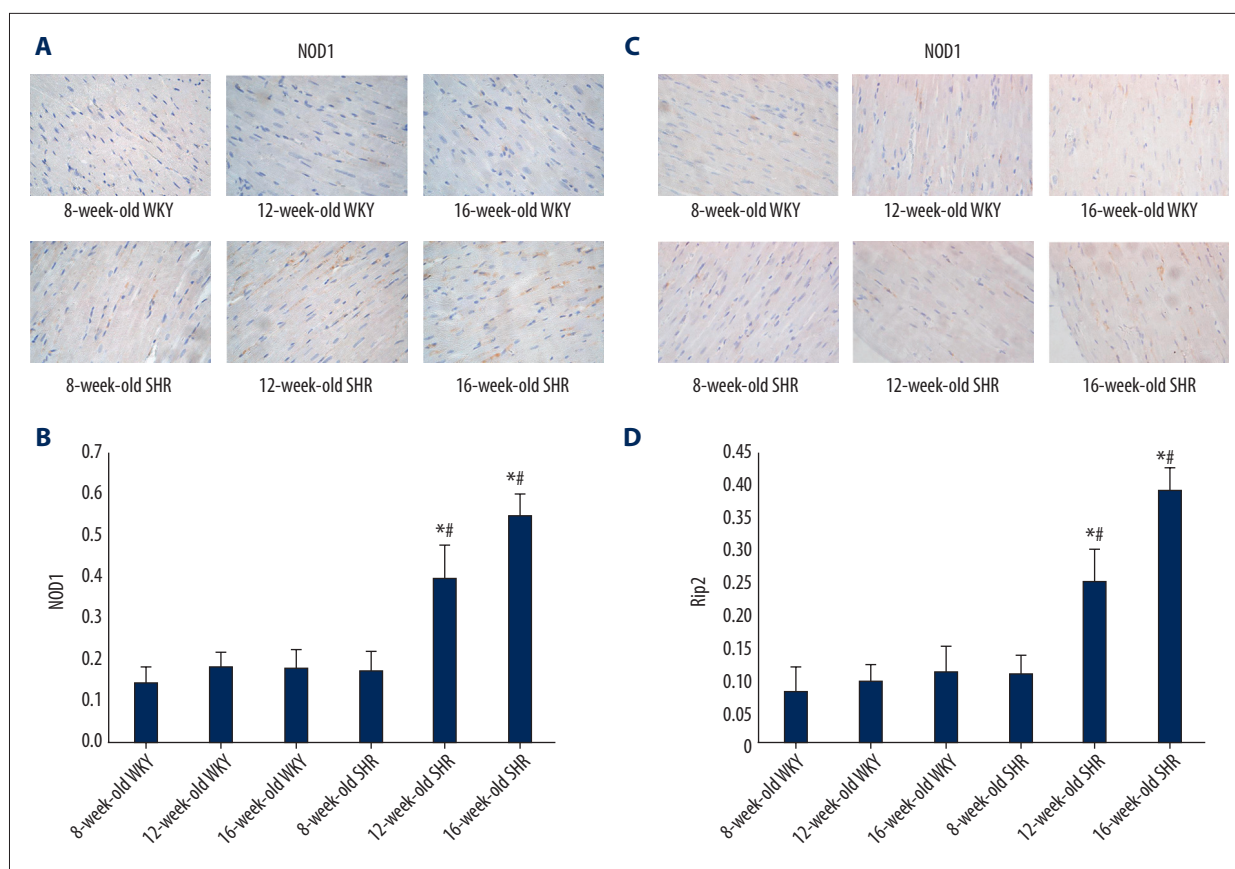
Figure 7. (**A, C**) Immunohistochemical staining showing the expression of the NOD1 and Rip2 proteins in the myocardial tissue from rats of different ages. (**B, D**) Semi-quantitative analysis of the expression of the NOD1 and Rip2 proteins in the myocardium from rats of different ages measured using immunohistochemical staining. * $P<0.05$ compared with WKY rats of the same age, and # $P<0.05$ compared with 8-week-old SHRs. NOD1 – nucleotide-binding oligomerization domain 1; Rip2 – receptor-interacting protein 2; SHRs – spontaneously hypertensive rats; WKY – Wistar-Kyoto.

of the SHR-H group increased by 77.6%, and the CVF% of the SHR-I group decreased by 68.9% ($P<0.05$).

Detection of the serum levels of the inflammatory factor IL-1 in rats using an ELISA

An ELISA kit was used to detect IL-1 levels in rat serum samples. As shown in Figure 10A, significantly higher levels of the inflammatory factor IL-1 were detected in 16-week-old SHRs than in WKY rats and 8- and 12-week-old SHRs. Significantly higher IL-1 levels were detected in 12-week-old SHRs than in 8-week-old SHRs and WKY rats. The results were statistically significant ($P<0.05$).

After treatment with the agonist and inhibitor, the levels of IL-1 in each experimental group were measured, as shown in Figure 10B. Compared with SHR-C group, significantly higher serum IL-1 levels were detected in the SHR-H group and significantly lower serum IL-1 levels were detected in the SHR-I

group ($P<0.05$). A significant difference was not observed between the SHR-C group and the normal saline group ($P>0.05$).

Discussion

Hypertension has the characteristics of a high incidence, high mortality rate, and high disability rate in our country due to its serious complications, and it seriously endangers public health. Long-term hypertension changes the structure and function of the heart, brain, kidney, and vascular system. The heart, an important target organ of hypertension, exhibits the characteristic pathological changes of left atrial enlargement and left ventricular hypertrophy, which may cause cardiac diastolic and systolic dysfunction, such as symptomatic heart failure and arrhythmia [19]. In the late stage of hypertension, cardiomyocytes undergo apoptosis and necrosis, which leads to myocardial remodeling, the enlargement of the heart and a decrease in the systolic function [20].
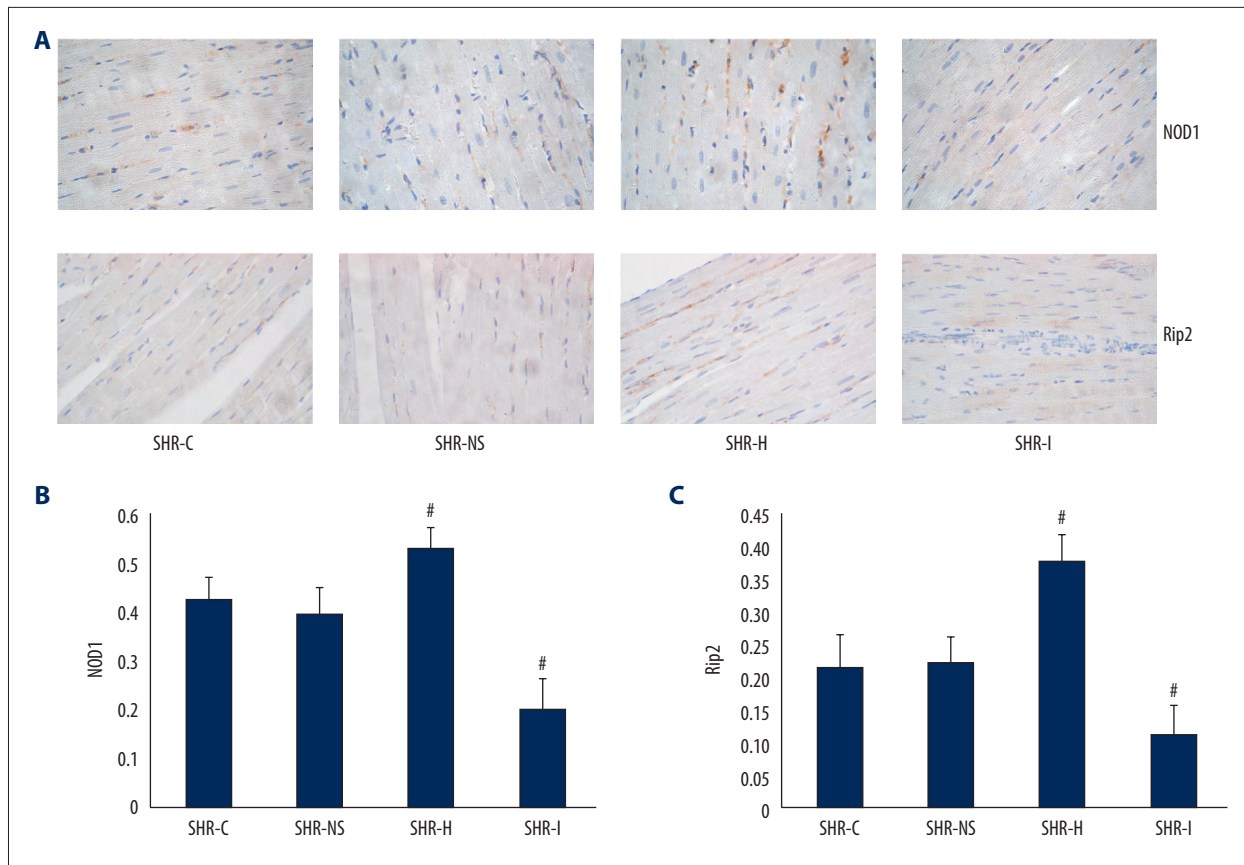
Figure 8. (**A**) Immunohistochemical staining showing the expression of the NOD1 and Rip2 proteins in the myocardium. (**B, C**) Semi-quantitative analysis of the expression of the NOD1 and Rip2 proteins in the myocardium from rats in each group measured using immunohistochemical staining. * $P<0.05$ compared with the SHR-C group, and # $P<0.05$ compared with the SHR-NS group. NOD1 – nucleotide-binding oligomerization domain 1; Rip2 – receptor-interacting protein 2; SHRs – spontaneously hypertensive rats; SHR-C group – control group; SHR-NS group – saline injection group.

Blood pressure increases with age in SHRs, and hypertension occurs 3 to 4 months after birth [21]. The pathological changes caused by hypertension appear during the development of the disease, including ventricular hypertrophy [22]. Therefore, SHRs are a useful model for studies of the pathogenesis of hypertension. In the present study, the blood pressure of SHRs and WKY rats increased with age, but the blood pressure of SHRs was significantly higher than WKY rats of the same age (Figure 1A, 1B). Based on H&E staining, an increased number of collagen fibers in a disordered arrangement between myocardial cells, an increased number of myocardial cells, partially broken fibers, cytosolic lysis and necrosis, and a blurred boundary were observed in 16-week-old SHRs (Figure 4A). The IVST and LVPWT measured using echocardiography were significantly thicker in 16-week-old SHRs (Figure 2F, 2G). VG staining revealed a significant increase in the number of myocardial collagen and a disordered arrangement in SHRs (Figure 9A). The semiquantitative analysis of VG staining showed a 3.65 times higher CVF% in 16-week-old SHRs than in 8-week-old SHRs and a 2.3 times higher CVF% in 12-week-old SHRs than

in 8-week-old SHRs (Figure 9C). Thus, left ventricular hypertrophy appeared during the development of hypertension in SHRs.

Innate immunity is a series of natural defense mechanisms that developed during the long-term evolution of organisms. The innate immune response is activated by PRR to recognize PAMPs and injury-associated molecular patterns (damage-associated molecular pattern, DAMP), thus generating immune effects [7]. On the one hand, immune cells and innate immune signaling molecules in the cardiovascular system upregulate the expression of immune response-related factors and participate in myocardial remodeling; on the other hand, these signals may be transduced by the classical signaling pathway of myocardial remodeling, such as mitogen-activated protein kinase, serine/threonine kinase, and calcium signaling pathways, resulting in myocardial remodeling [23]. Therefore, the innate immune response is also involved in myocardial remodeling. NLR is an important family of innate immune pattern recognition receptors that play an important regulatory role in cardiovascular disease [24–26]. A NOD1-deficient mouse model
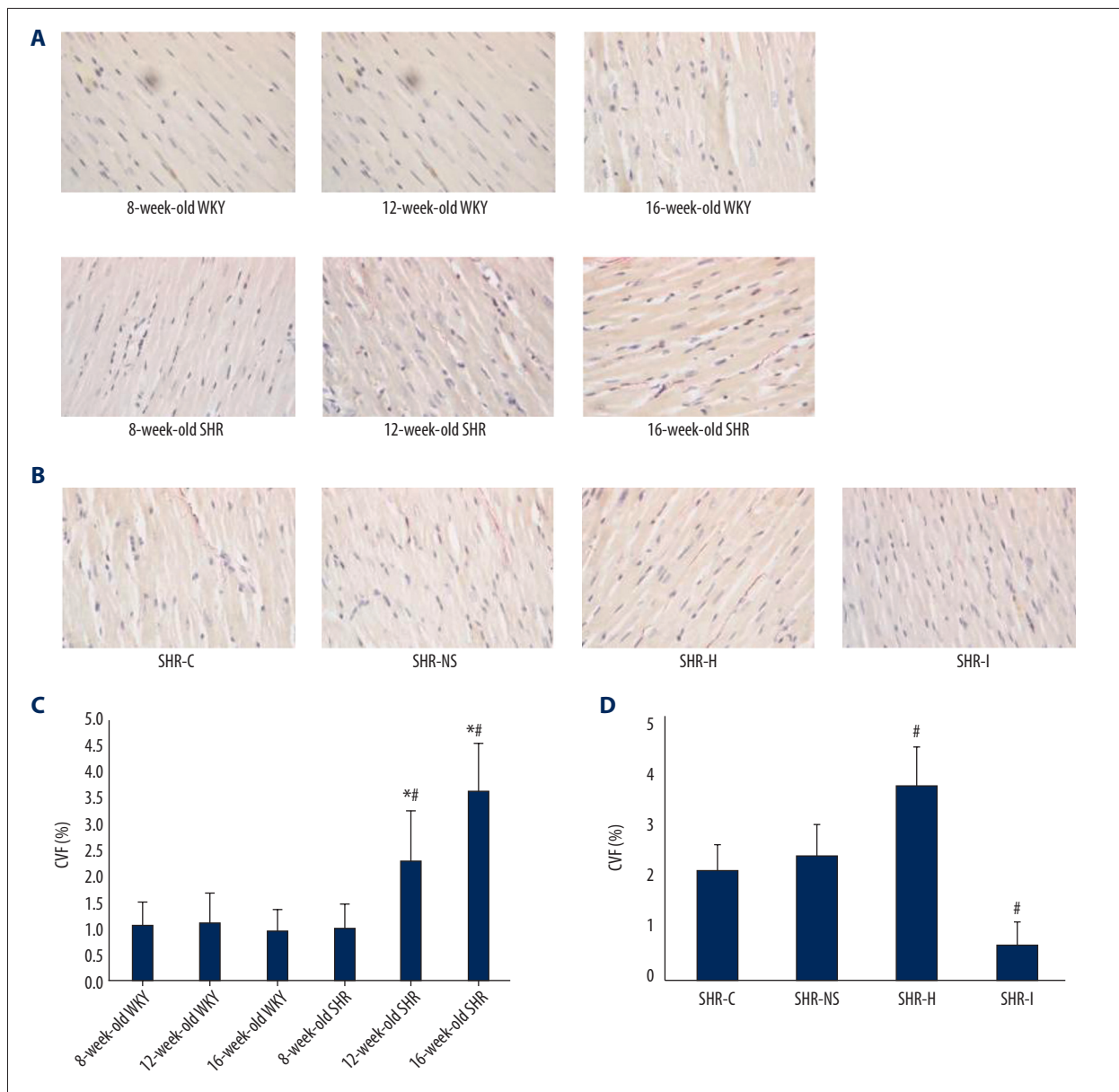
Figure 9. (**A**) VG staining in rats of different ages. (**B**) VG staining in rats from each group. (**C**) Semi-quantitative analysis of VG staining in rats of different ages. * $P<0.05$ compared with WKY rats of the same age, and # $P<0.05$ compared with 8-week-old SHRs. (**D**) Semi-quantitative analysis of VG staining in rats from each group. # $P<0.05$ compared with the SHR-C group. VG – Van Gieson; WKY – Wistar-Kyoto; SHRs – spontaneously hypertensive rats; SHR-C group – control group.

of heart failure improved the β-adrenergic modulation of Ca²⁺ signaling, and the innate immune receptor NOD1 plays an import role in heart failure [27]. In contrast, NOD2 is a negative regulator of hypertensive ventricular remodeling. After aortic banding surgery, the expression of NOD2 in wild type mice was upregulated, while ventricular remodeling in NOD2⁻/⁻ mice was aggravated [28]. Activation of NOD1 is often accompanied by activation of downstream factor Rip2, and many studies have confirmed that the increase of Rip2 expression was used to express the activation of downstream factors of

NOD1 [10,29–31]. In the present study, we detected the expression of NOD1 and Rip2 in the rat myocardium using RT-PCR, western blotting, and immunohistochemistry. The expression of NOD1 and Rip2 in the myocardial tissue of SHRs increased with aging, and higher expression was observed in the myocardium of 16-week-old SHRs than in WKY rats and 8-week-old SHRs, suggesting that the NOD1/Rip2 signaling pathway may be involved in myocardial remodeling in SHRs.
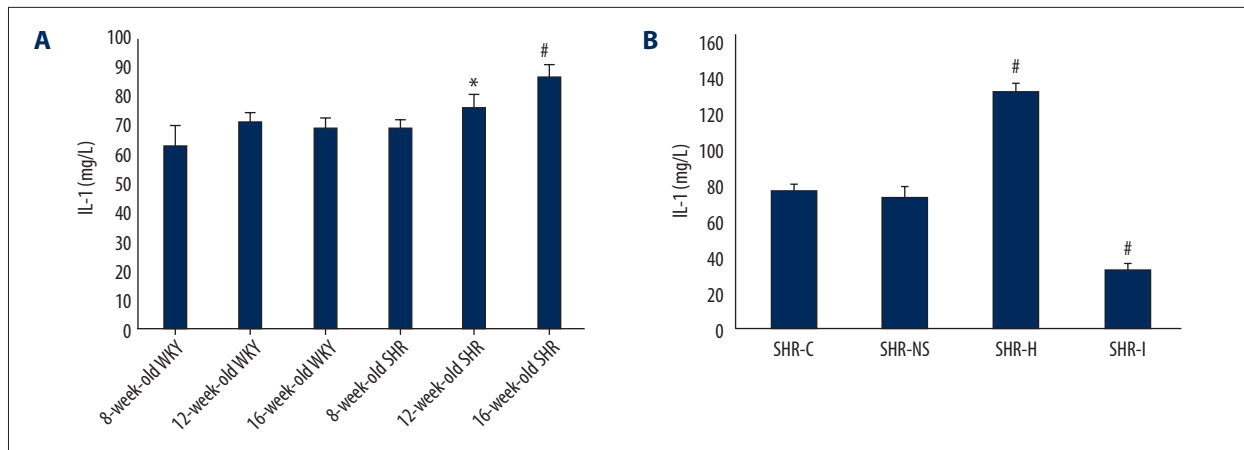
Figure 10. (**A**) Serum levels of IL-1 in SHRs and WKY rats were measured using an ELISA. * *P*<0.05 compared with WKY rats and 8-week-old SHRs, # *P*<0.05 compared with WKY rats and 8- and 12-week-old SHRs. (**B**) Serum IL-1 levels in rats from each group were detected using an ELISA. # *P*<0.05 compared with the SHR-C group. SHRs – spontaneously hypertensive rats; WKY – Wistar-Kyoto; ELISA – enzyme-linked immunosorbent assay; IL-1 – interleukin-1; SHR-C group – control group.

We treated SHRs with iE-DAP, an agonist of the NOD1 receptor, and ML130, an inhibitor of the NOD1 receptor, to modulate the activity of the NOD1/Rip2 signaling pathway and further verify its effect on myocardial remodeling in SHRs. Compared with the control group, NOD1 and Rip2 expression was upregulated in the myocardial tissue of SHRs intraperitoneally injected with the NOD1 agonist iE-DAP, as detected using real-time RT-PCR, western blotting, and immunohistochemistry. Moreover, blood pressure was significantly increased, and myocardial remodeling was obviously manifested as a marked enlargement of cardiac myocytes, structural deterioration, an increase in myocardial collagen volume fraction, and thickening of the IVST and LVPWT. In contrast, NOD1 and Rip2 expression were downregulated in SHRs intraperitoneally injected with the NOD1 inhibitor ML130, blood pressure was significantly decreased, and myocardial remodeling was delayed. A significant finding of our study is that the NOD1 inhibitor decreased blood pressure and improved myocardial remodeling.

The mechanism of myocardial hypertrophy is related not only to the mechanical stress response caused by elevated blood pressure but also to the effects of neurohormones, growth factors, and cytokines [32]. The mechanical pressure produced by an elevated blood pressure also activates many intracellular signaling pathways through receptors on cardiac cell membrane, which may increase the production of fibrin products and induce cardiac hypertrophy [33]. Many studies have shown the relationship between NOD1 and inflammatory reactions. Among the NLR family members, NOD proteins induce specific inflammatory responses [34,35]. NOD1 participates in inflammatory responses after renal ischemia reperfusion injury [36]. NOD1 activity promotes chronic inflammatory disorders [37,38] in individuals with several diseases through NF-kB activation and cytokine production [39,40].

In the present study, serum levels of the inflammatory factor IL-1 increased in SHRs with age, and the NOD1 agonist increased the concentration of IL-1, while the NOD1 inhibitor decreased the concentration of IL-1. IL-1 is an important cytokine involved in the immune and inflammatory responses. The IL-1 family induces the expression of inflammatory and autoimmune-related genes that play an important role in the inflammatory response and immune process of many diseases [41–43]. Dalekos et al. [44] were the first to observe a significant increase in the serum IL-1 β level in patients with essential hypertension, suggesting that the cytokine IL-1β may be related to hypertension. Krishnan proposed that IL-1 is closely related to the pathogenesis of hypertension [45]. An increase in serum IL-1 levels is usually accompanied by the proliferation of extracellular matrix (ECM) and myocardial interstitial fibrosis [46]. IL-1 is involved in the development of myocardial remodeling after myocardial infarction, and it promotes myocardial hypertrophy in the pathogenesis of heart failure [47]. *In vitro* experiments in which myocardial fibroblasts were stimulated with IL-1β indicated that this cytokine promotes fibronectin production [48], reduces collagen synthesis, increases matrix metalloproteinase activity [49], promotes ECM deposition, and subsequently leads to myocardial fibrosis. After stimulation with IL-1β, the density of angiotensin II type 1 receptor in cultured myocardial fibroblasts was increased, and angiotensin II subsequently promoted fibrosis [50]. Our study confirmed that the activation of NOD1/Rip2 signaling in SHRs increased the levels of the downstream cytokine IL-1, which might further aggravate myocardial remodeling.

Conclusion

In conclusion, the NOD1/Rip2 signaling pathway is involved in regulating blood pressure and myocardial remodeling in SHRs, and inhibition of the NOD1/Rip2 signaling pathway reduces blood pressure and prevents myocardial remodeling in SHRs. Moreover, IL-1 is involved in the NOD1/Rip2-induced effects. The blockade of the NOD1/Rip2 signaling pathway may become a new target for the prevention and treatment of hypertension and the protection of target organs in the future.

References:

1. Giles TD, Berk BC, Black HR et al: Expanding the definition and classification of hypertension. J Clin Hypertens, 2005; 7(9): 505–12

2. Marian AJ: Experimental therapies in hypertrophic cardiomyopathy. J Cardiovasc Transl Res, 2009; 2(4): 483–92

3. Amani H, Mostafavi E, Arzaghi H et al: Three-dimensional graphene foams: synthesis, properties, biocompatibility, biodegradability, and applications in tissue engineering. ACS Biomater Sci Eng, 2019; 5: 193–214

4. Ettehad D, Emdin CA, Kiran A et al: Blood pressure lowering for prevention of cardiovascular disease and death: A systematic review and meta-analysis. Lancet, 2016; 387(10022): 957–67

5. Ting JP, Duncan JA, Lei Y: How the noninflammasome NLRs function in the innate immune system. Science, 2010; 327: 286–90

6. Linde A, Mosier D, Blecha F et al: Innate immunity and inflammation: New frontiers in comparative cardiovascular pathology. Cardiovasc Res, 2007; 73(1): 26–36

7. Brubaker SW, Bonham KS, Zanoni I et al: Innate immune pattern recognition: A cell biological perspective. Annu Rev Immunol, 2015; 33: 257–90

8. Bullón P, Alcocer-Gómez E, Carrión AM et al: AMPK phosphorylation modulates pain by activation of NLRP3 Inflammasome. Antioxid Redox Signal, 2016; 24(3): 157–70

9. Monnerat G, Alarcón ML, Vasconcellos LR et al: Macrophage -dependent IL-1beta production induces cardiac arrhythmias in diabetic mice. Nat Commun, 2016; 7: 13344

10. Val-Blasco A, Piedras MJGM, Ruiz-Hurtado G et al: Role of NOD1 in heart failure progression via regulation of Ca²⁺ handling. J Am Coll Cardiol, 2017; 69(4): 423–33

11. Balamayooran T, Balamayooran G, Jeyaseelan S: Review: Toll-like receptors and NOD-like receptors in pulmonary antibacterial immunity. Innate Immunity, 2010; 16(3): 201–10

12. Fernández-Velasco M, Prieto P, Terrón V et al: NOD1 activation induces cardiac dysfunction and modulates cardiac fibrosis and cardiomyocyte apoptosis. PLoS One, 2012; 7(9): e45260

13. Delgado C, Ruiz-Hurtado G, Gómez-Hurtado N et al: NOD1, a new player in cardiac function and calcium handling. Cardiovasc Res, 2015; 106(3): 375–86

14. Park JH, Kim YG, McDonald C et al: RICK/RIP2 mediates innate immune responses induced through Nod1 and Nod2 but not TLRs. J Immunol, 2007; 178(4): 2380–86

15. da Silva Correia J, Miranda Y et al: Regulation of Nod1-mediated signaling pathways. Cell Death Differ, 2007; 14(4): 830–39

16. Caruso R, Warner N, Inohara N et al: NOD1 and NOD2: Signaling, host defense, and inflammatory disease. Immunity, 2014; 41(6): 898–908

17. Peterson LW, Artis D: Intestinal epithelial cells: Regulators of barrier function and immune homeostasis. Nat Rev Immunol, 2014; 14(3): 141–53

18. Philpott DJ, Sorbara MT, Robertson SJ et al: NOD proteins: Regulators of inflammation in health and disease. Nat Rev Immunol, 2014; 14(1): 9–23

19. Drazner MH: The progression of hypertensive heart disease. Circulation, 2011; 123(3): 327–34

20. Gupta PK, DiPette DJ, Supowit SC: Protective effect of resveratrol against pressure overload-induced heart failure. Food Sci Nutr, 2014; 2(3): 218–29

21. Wu YT, Qian ZQ, Fu S et al: Icariside II improves left ventricular remodeling in spontaneously hypertensive rats by inhibiting the ASK1-JNK/p38 signaling pathway. Eur J Pharmacol, 2018; 819: 68–79

22. Abbate A, Scarpa S, Santini D et al: Myocardial expression of surviving, an apoptosis inhibitor, in aging and heart failure. An experimental study in the spontaneously hypertensive rats. Int J Cardiol, 2006; 111(3): 371–76

23. Zhang XJ, Zhang P, Li H: Interferon regulatory factor signalings in cardiometabolic diseases. Hypertension, 2015; 66(2): 222–47

24. Nishio H, Kanno S, Onoyama S et al: Nod1 ligands induce site-specific vascular inflammation. Arterioscler Throm Vasc Biol, 2011; 31(5): 1093–99

25. Moreno L, McMaster SK, Gatheral T et al: Nucleotide oligomerization domain 1 is a dominant pathway for NOS2 induction in vascular smooth muscle cells: Comparison with Toll-like receptor 4 responses in macrophages. Br J Pharmacol, 2010; 160(8): 1997–2007

26. Duewell P, Kono H, Rayner KJ et al: NLRP3 inflammasomes are required for atherogenesis and activated by cholesterol crystals. Nature, 2010; 464(7293): 1357–61

27. Val-Blasco A, Navarro-García JA, Tamayo M et al: Deficiency of NOD1 improves the β-adrenergic modulation of Ca²⁺ handling in a mouse model of heart failure. Front Physiol, 2018; 9: 702

28. Zong J, Salim M, Zhou H et al: NOD2 deletion promotes cardiac hypertrophy and fibrosis induced by pressure overload. Lab Invest, 2013; 93(10): 1128–36

29. Zhu L, Wang Y, Zhu Y et al: Expression of NOD1 and downstream factors in placenta, fetal membrane and plasma from pregnancies with premature rupture of membranes and their significance. Int J Clin Exp Pathol, 2018; 11(12): 5745–54

30. Bist P, Dikshit N, Koh TH et al: The Nod1, Nod2, and Rip2 axis contributes to host immune defense against intracellular *Acinetobacter baumannii*. Infection, 2014; 82(3): 1112–22

31. Chan LP, Wang LF, Chiang FY et al: IL-8 promotes HNSCC progression on CXCR1/2-mediated NOD1/RIP2 signaling pathway. Oncotarget, 2016; 7(38): 61820–31

32. Diez J, Frohlich ED: A translational approach to hypertensive heart disease. Hypertension, 2010; 55(1): 1–8

33. Rohini A, Agrawal N, Koyani CN et al: Molecular targets and regulators of Cardiac hypertrophy. Pharmacol Res, 2010; 61(4): 269–80

34. Kanneganti TD, Lamkanfi M, Nunez G: Intracellular NOD-like receptors in host defense and disease. Immunity, 2007; 27(4): 549–59

35. Fritz JH, Ferrero RL, Philpott DJ et al: Nod-like proteins in immunity, inflammation and disease. Nat Immunol, 2006; 7(12): 1250–57

36. Kasimsetty SG, Hawkes A, Barekatain K et al: TLR2 and NODs1 and 2 cooperate in inflammatory responses associated with renal ischemia reperfusion injury. Transpl Immunol, 2019; 58: 101260

37. Hysi P, Kabesch M, Moffatt MF et al: NOD1 variation, immunoglobulin E and asthma. Hum Mol Genet, 2005; 14(7): 935–41

38. Weidinger S, Klopp N, Rummler L et al: Association of NOD1 polymorphisms with atopic eczema and related phenotypes. J Allergy Clin Immunol, 2005; 116(1): 177–84

39. da Silva Correia J, Miranda Y, Austin-Brown N et al: Nod1-dependent control of tumor growth. Proc Natl Acad Sci USA, 2006; 103(6): 1840–45

40. Girardin SE, Tournebize R, Mavris M et al: CARD4/Nod1 mediates NF-κB and JNK activation by invasive *Shigella flexneri*. EMBO Rep, 2001; 2(8): 736–42

41. Mantovani A, Dinarello CA, Molgora M et al: Interleukin-1 and related cytokines in the regulation of inflammation and immunity. Immunity, 2019; 50(4): 778–95

42. Sims JE, Smith DE: The IL-1 family: Regulators of immunity. Nat Rev Immunol, 2010; 10(2): 89–102

43. Muñoz-Wolf N, Lavelle EC: A guide to IL-1 family cytokines in adjuvanticity. FEBS J, 2018; 285(13): 2377–401

44. Dalekos GN, Elisaf M, Bairaktari E et al: Increased serum levels of interleukin-1beta in the systemic circulation of patients with essential hypertension: Additional risk factor for atherogenesis in hypertensive patients? J Lab Clin Med, 1997; 129(3): 300–8

45. Krishnan SM, Sobey CG, Latz E et al: IL-1β and IL-18: Inflammatory markers or mediators of hypertension? Br J Pharmacol, 2014; 171(24): 5589–602

46. Cain BS, Meldrum DR, Dinarello CA et al: Tumor necrosis factor-alpha and interleukin-l beta synergistically depress human myocardial function. Crit Care Med, 1999; 27(7): 1309–18

47. Bujak M, Frangogiannis NG: The role of Interleukin-1 in the pathogenesis of heart disease. Arch Immunol Ther Exp, 2009; 57(3): 165–76

48. Fernández L, Mosquera JA: Interleukin-l increases fibronectin production by cultured rat cardiac fibroblasts. Pathobiology, 2002; 70(4): 191–96

49. Siwik DA, Chang DL, Colucci WS: Interleukin-1 beta and tumor necrosis factor-alpha decrease collagen synthesis and increase matrix metalloproteinase activity in cardiac fibroblasts *in vitro*. Circ Res, 2000; 86(12): 1259–65

50. Gurantz D, Cowling RT, Varki N et al: IL-1β and TNF-α upregulate angiotensin II type 1 (AT1) receptors on cardiac fibroblasts and are associated with increased AT1 density in the post-MI heart. J Mol Cell Cardiol, 2005; 38(3): 505–15